

Small Angle Muon and Bottom Quark Production in $p\bar{p}$ Collisions at $\sqrt{s} = 1.8$ TeV

B. Abbott,⁴⁵ M. Abolins,⁴² V. Abramov,¹⁸ B.S. Acharya,¹¹ I. Adam,⁴⁴ D.L. Adams,⁵⁴
M. Adams,²⁸ S. Ahn,²⁷ V. Akimov,¹⁶ G.A. Alves,² N. Amos,⁴¹ E.W. Anderson,³⁴
M.M. Baarmand,⁴⁷ V.V. Babintsev,¹⁸ L. Babukhadia,²⁰ A. Baden,³⁸ B. Baldin,²⁷
S. Banerjee,¹¹ J. Bantly,⁵¹ E. Barberis,²¹ P. Baringer,³⁵ J.F. Bartlett,²⁷ A. Belyaev,¹⁷
S.B. Beri,⁹ I. Bertram,¹⁹ V.A. Bezzubov,¹⁸ P.C. Bhat,²⁷ V. Bhatnagar,⁹
M. Bhattacharjee,⁴⁷ G. Blazey,²⁹ S. Blessing,²⁵ P. Bloom,²² A. Boehnlein,²⁷ N.I. Bojko,¹⁸
F. Borchering,²⁷ C. Boswell,²⁴ A. Brandt,²⁷ R. Breedon,²² G. Briskin,⁵¹ R. Brock,⁴²
A. Bross,²⁷ D. Buchholz,³⁰ V.S. Burtovoi,¹⁸ J.M. Butler,³⁹ W. Carvalho,³ D. Casey,⁴²
Z. Casilum,⁴⁷ H. Castilla-Valdez,¹⁴ D. Chakraborty,⁴⁷ K.M. Chan,⁴⁶ S.V. Chekulaev,¹⁸
W. Chen,⁴⁷ D.K. Cho,⁴⁶ S. Choi,¹³ S. Chopra,²⁵ B.C. Choudhary,²⁴ J.H. Christenson,²⁷
M. Chung,²⁸ D. Claes,⁴³ A.R. Clark,²¹ W.G. Cobau,³⁸ J. Cochran,²⁴ L. Coney,³²
W.E. Cooper,²⁷ D. Coppage,³⁵ C. Cretsinger,⁴⁶ D. Cullen-Vidal,⁵¹ M.A.C. Cummings,²⁹
D. Cutts,⁵¹ O.I. Dahl,²¹ K. Davis,²⁰ K. De,⁵² K. Del Signore,⁴¹ M. Demarteau,²⁷
D. Denisov,²⁷ S.P. Denisov,¹⁸ H.T. Diehl,²⁷ M. Diesburg,²⁷ G. Di Loreto,⁴² P. Draper,⁵²
Y. Ducros,⁸ L.V. Dudko,¹⁷ S.R. Dugad,¹¹ A. Dyshkant,¹⁸ D. Edmunds,⁴² J. Ellison,²⁴
V.D. Elvira,⁴⁷ R. Engelmann,⁴⁷ S. Eno,³⁸ G. Eppley,⁵⁴ P. Ermolov,¹⁷ O.V. Eroshin,¹⁸
J. Estrada,⁴⁶ H. Evans,⁴⁴ V.N. Evdokimov,¹⁸ T. Fahland,²³ M.K. Fatyga,⁴⁶ S. Feher,²⁷
D. Fein,²⁰ T. Ferbel,⁴⁶ H.E. Fisk,²⁷ Y. Fisyrak,⁴⁸ E. Flattum,²⁷ G.E. Forden,²⁰ M. Fortner,²⁹
K.C. Frame,⁴² S. Fuess,²⁷ E. Gallas,²⁷ A.N. Galyaev,¹⁸ P. Gattung,²⁴ V. Gavrilo, ¹⁶
T.L. Geld,⁴² R.J. Genik II,⁴² K. Genser,²⁷ C.E. Gerber,²⁷ Y. Gershtein,⁵¹ B. Gibbard,⁴⁸
G. Ginther,⁴⁶ B. Gobbi,³⁰ B. Gómez,⁵ G. Gómez,³⁸ P.I. Goncharov,¹⁸ J.L. González Solís,¹⁴
H. Gordon,⁴⁸ L.T. Goss,⁵³ K. Gounder,²⁴ A. Goussiou,⁴⁷ N. Graf,⁴⁸ P.D. Grannis,⁴⁷
D.R. Green,²⁷ J.A. Green,³⁴ H. Greenlee,²⁷ S. Grinstein,¹ P. Grudberg,²¹ S. Grünendahl,²⁷
G. Guglielmo,⁵⁰ J.A. Guida,²⁰ J.M. Guida,⁵¹ A. Gupta,¹¹ S.N. Gurzhiev,¹⁸ G. Gutierrez,²⁷
P. Gutierrez,⁵⁰ N.J. Hadley,³⁸ H. Haggerty,²⁷ S. Hagopian,²⁵ V. Hagopian,²⁵ K.S. Hahn,⁴⁶
R.E. Hall,²³ P. Hanlet,⁴⁰ S. Hansen,²⁷ J.M. Hauptman,³⁴ C. Hays,⁴⁴ C. Hebert,³⁵
D. Hedin,²⁹ A.P. Heinson,²⁴ U. Heintz,³⁹ R. Hernández-Montoya,¹⁴ T. Heuring,²⁵
R. Hirsosky,²⁸ J.D. Hobbs,⁴⁷ B. Hoeneisen,⁶ J.S. Hoftun,⁵¹ F. Hsieh,⁴¹ Tong Hu,³¹ A.S. Ito,²⁷
S.A. Jerger,⁴² R. Jesik,³¹ T. Joffe-Minor,³⁰ K. Johns,²⁰ M. Johnson,²⁷ A. Jonckheere,²⁷
M. Jones,²⁶ H. Jöstlein,²⁷ S.Y. Jun,³⁰ S. Kahn,⁴⁸ D. Karmanov,¹⁷ D. Karmgard,²⁵
R. Kehoe,³² S.K. Kim,¹³ B. Klima,²⁷ C. Klopfenstein,²² B. Knuteson,²¹ W. Ko,²²
J.M. Kohli,⁹ D. Koltick,³³ A.V. Kostritskiy,¹⁸ J. Kotcher,⁴⁸ A.V. Kotwal,⁴⁴ A.V. Kozelov,¹⁸
E.A. Kozlovsky,¹⁸ J. Krane,³⁴ M.R. Krishnaswamy,¹¹ S. Krzywdzinski,²⁷ M. Kubantsev,³⁶
S. Kuleshov,¹⁶ Y. Kulik,⁴⁷ S. Kunori,³⁸ F. Landry,⁴² G. Landsberg,⁵¹ A. Leflat,¹⁷ J. Li,⁵²
Q.Z. Li,²⁷ J.G.R. Lima,³ D. Lincoln,²⁷ S.L. Linn,²⁵ J. Linnemann,⁴² R. Lipton,²⁷ J.G. Lu,⁴
A. Lucotte,⁴⁷ L. Lueking,²⁷ A.K.A. Maciel,²⁹ R.J. Madaras,²¹ R. Madden,²⁵
L. Magaña-Mendoza,¹⁴ V. Manankov,¹⁷ S. Mani,²² H.S. Mao,⁴ R. Markeloff,²⁹
T. Marshall,³¹ M.I. Martin,²⁷ R.D. Martin,²⁸ K.M. Mauritz,³⁴ B. May,³⁰ A.A. Mayorov,¹⁸
R. McCarthy,⁴⁷ J. McDonald,²⁵ T. McKibben,²⁸ J. McKinley,⁴² T. McMahan,⁴⁹
H.L. Melanson,²⁷ M. Merkin,¹⁷ K.W. Merritt,²⁷ C. Miao,⁵¹ H. Miettinen,⁵⁴ A. Mincer,⁴⁵

C.S. Mishra,²⁷ N. Mokhov,²⁷ N.K. Mondal,¹¹ H.E. Montgomery,²⁷ M. Mostafa,¹
H. da Motta,² F. Nang,²⁰ M. Narain,³⁹ V.S. Narasimham,¹¹ A. Narayanan,²⁰ H.A. Neal,⁴¹
J.P. Negret,⁵ P. Nemethy,⁴⁵ D. Norman,⁵³ L. Oesch,⁴¹ V. Oguri,³ N. Oshima,²⁷ D. Owen,⁴²
P. Padley,⁵⁴ A. Para,²⁷ N. Parashar,⁴⁰ Y.M. Park,¹² R. Partridge,⁵¹ N. Parua,⁷
M. Paterno,⁴⁶ B. Pawlik,¹⁵ J. Perkins,⁵² M. Peters,²⁶ R. Piegaiia,¹ H. Piekarczyk,²⁵
Y. Pischalnikov,³³ B.G. Pope,⁴² H.B. Prosper,²⁵ S. Protopopescu,⁴⁸ J. Qian,⁴¹
P.Z. Quintas,²⁷ R. Raja,²⁷ S. Rajagopalan,⁴⁸ O. Ramirez,²⁸ N.W. Reay,³⁶ S. Reucroft,⁴⁰
M. Rijssenbeek,⁴⁷ T. Rockwell,⁴² M. Roco,²⁷ P. Rubinov,³⁰ R. Ruchti,³² J. Rutherford,²⁰
A. Sánchez-Hernández,¹⁴ A. Santoro,² L. Sawyer,³⁷ R.D. Schamberger,⁴⁷ H. Schellman,³⁰
J. Sculli,⁴⁵ E. Shabalina,¹⁷ C. Shaffer,²⁵ H.C. Shankar,¹¹ R.K. Shivpuri,¹⁰ D. Shpakov,⁴⁷
M. Shupe,²⁰ R.A. Sidwell,³⁶ H. Singh,²⁴ J.B. Singh,⁹ V. Sirotenko,²⁹ P. Slattery,⁴⁶
E. Smith,⁵⁰ R.P. Smith,²⁷ R. Snihur,³⁰ G.R. Snow,⁴³ J. Snow,⁴⁹ S. Snyder,⁴⁸ J. Solomon,²⁸
X.F. Song,⁴ M. Sosebee,⁵² N. Sotnikova,¹⁷ M. Souza,² N.R. Stanton,³⁶ G. Steinbrück,⁵⁰
R.W. Stephens,⁵² M.L. Stevenson,²¹ F. Stichelbaut,⁴⁸ D. Stoker,²³ V. Stolin,¹⁶
D.A. Stoyanova,¹⁸ M. Strauss,⁵⁰ K. Streets,⁴⁵ M. Strovink,²¹ A. Sznajder,³ P. Tamburello,³⁸
J. Tarazi,²³ M. Tartaglia,²⁷ T.L.T. Thomas,³⁰ J. Thompson,³⁸ D. Toback,³⁸ T.G. Trippe,²¹
P.M. Tuts,⁴⁴ V. Vaniev,¹⁸ N. Varelas,²⁸ E.W. Varnes,²¹ A.A. Volkov,¹⁸ A.P. Vorobiev,¹⁸
H.D. Wahl,²⁵ J. Warchol,³² G. Watts,⁵¹ M. Wayne,³² H. Weerts,⁴² A. White,⁵²
J.T. White,⁵³ J.A. Wightman,³⁴ S. Willis,²⁹ S.J. Wimpenny,²⁴ J.V.D. Wirjawan,⁵³
J. Womersley,²⁷ D.R. Wood,⁴⁰ R. Yamada,²⁷ P. Yamin,⁴⁸ T. Yasuda,²⁷ P. Yepes,⁵⁴
K. Yip,²⁷ C. Yoshikawa,²⁶ S. Youssef,²⁵ J. Yu,²⁷ Y. Yu,¹³ M. Zanabria,⁵ Z. Zhou,³⁴
Z.H. Zhu,⁴⁶ M. Zielinski,⁴⁶ D. Zieminska,³¹ A. Zieminski,³¹ V. Zutshi,⁴⁶ E.G. Zverev,¹⁷
and A. Zylberstejn⁸

(DØ Collaboration)

¹ *Universidad de Buenos Aires, Buenos Aires, Argentina*

² *LAFEX, Centro Brasileiro de Pesquisas Físicas, Rio de Janeiro, Brazil*

³ *Universidade do Estado do Rio de Janeiro, Rio de Janeiro, Brazil*

⁴ *Institute of High Energy Physics, Beijing, People's Republic of China*

⁵ *Universidad de los Andes, Bogotá, Colombia*

⁶ *Universidad San Francisco de Quito, Quito, Ecuador*

⁷ *Institut des Sciences Nucléaires, IN2P3-CNRS, Université de Grenoble 1, Grenoble, France*

⁸ *DAPNIA/Service de Physique des Particules, CEA, Saclay, France*

⁹ *Panjab University, Chandigarh, India*

¹⁰ *Delhi University, Delhi, India*

¹¹ *Tata Institute of Fundamental Research, Mumbai, India*

¹² *Kyungshung University, Pusan, Korea*

¹³ *Seoul National University, Seoul, Korea*

¹⁴ *CINVESTAV, Mexico City, Mexico*

¹⁵ *Institute of Nuclear Physics, Kraków, Poland*

¹⁶ *Institute for Theoretical and Experimental Physics, Moscow, Russia*

¹⁷ *Moscow State University, Moscow, Russia*

¹⁸ *Institute for High Energy Physics, Protvino, Russia*

¹⁹ *Lancaster University, Lancaster, United Kingdom*

²⁰ *University of Arizona, Tucson, Arizona 85721*

- ²¹*Lawrence Berkeley National Laboratory and University of California, Berkeley, California 94720*
- ²²*University of California, Davis, California 95616*
- ²³*University of California, Irvine, California 92697*
- ²⁴*University of California, Riverside, California 92521*
- ²⁵*Florida State University, Tallahassee, Florida 32306*
- ²⁶*University of Hawaii, Honolulu, Hawaii 96822*
- ²⁷*Fermi National Accelerator Laboratory, Batavia, Illinois 60510*
- ²⁸*University of Illinois at Chicago, Chicago, Illinois 60607*
- ²⁹*Northern Illinois University, DeKalb, Illinois 60115*
- ³⁰*Northwestern University, Evanston, Illinois 60208*
- ³¹*Indiana University, Bloomington, Indiana 47405*
- ³²*University of Notre Dame, Notre Dame, Indiana 46556*
- ³³*Purdue University, West Lafayette, Indiana 47907*
- ³⁴*Iowa State University, Ames, Iowa 50011*
- ³⁵*University of Kansas, Lawrence, Kansas 66045*
- ³⁶*Kansas State University, Manhattan, Kansas 66506*
- ³⁷*Louisiana Tech University, Ruston, Louisiana 71272*
- ³⁸*University of Maryland, College Park, Maryland 20742*
- ³⁹*Boston University, Boston, Massachusetts 02215*
- ⁴⁰*Northeastern University, Boston, Massachusetts 02115*
- ⁴¹*University of Michigan, Ann Arbor, Michigan 48109*
- ⁴²*Michigan State University, East Lansing, Michigan 48824*
- ⁴³*University of Nebraska, Lincoln, Nebraska 68588*
- ⁴⁴*Columbia University, New York, New York 10027*
- ⁴⁵*New York University, New York, New York 10003*
- ⁴⁶*University of Rochester, Rochester, New York 14627*
- ⁴⁷*State University of New York, Stony Brook, New York 11794*
- ⁴⁸*Brookhaven National Laboratory, Upton, New York 11973*
- ⁴⁹*Langston University, Langston, Oklahoma 73050*
- ⁵⁰*University of Oklahoma, Norman, Oklahoma 73019*
- ⁵¹*Brown University, Providence, Rhode Island 02912*
- ⁵²*University of Texas, Arlington, Texas 76019*
- ⁵³*Texas A&M University, College Station, Texas 77843*
- ⁵⁴*Rice University, Houston, Texas 77005*

Abstract

This Letter describes a measurement of the muon cross section originating from b quark decay in the forward rapidity range $2.4 < |y^\mu| < 3.2$ in $p\bar{p}$ collisions at $\sqrt{s} = 1.8$ TeV. The data used in this analysis were collected by the DØ experiment at the Fermilab Tevatron. We find that NLO QCD calculations underestimate b quark production by a factor of four in the forward rapidity region.

Measurements of b quark production at the Tevatron have provided valuable information in the study of perturbative QCD. Cross sections measured by both the DØ [1,2], and CDF [3] collaborations in the central rapidity region ($|y^b| < 1.5$) are systematically higher (by a factor of two to three) than the nominal values predicted by next-to-leading order (NLO) QCD [4]. Furthermore, discrepancies between some of the predicted and measured shapes of $b\bar{b}$ correlation distributions [5] indicate that the difference between data and QCD cannot be explained by a simple normalization factor.

CDF has recently measured the $b\bar{b}$ cross section in which one quark is produced in the forward pseudorapidity region ($1.8 < |\eta^b| < 2.6$) and the other in the central range ($|\eta^b| < 1.5$) [6]. This measurement is a factor of 2.4 higher than the NLO QCD prediction.

Our measurement of the forward cross section of muons originating from b quark decay extends these studies to the previously unexplored rapidity region ($2.4 < |y^\mu| < 3.2$), and provides further insights into the discrepancy between b quark production measurements and theoretical predictions.

Forward muons are measured by the DØ detector [7] using the Small Angle MUon Spectrometer (SAMUS) [8,9]. SAMUS consists of two identical systems, each with three drift tube stations and a 1.8 T magnetized iron toroid, on either side of the interaction region. The momentum resolution of this system varies from $\approx 19\%$ at 20 GeV/ c to $\approx 25\%$ at 100 GeV/ c . Muons reaching the SAMUS chambers traverse approximately 20 interaction lengths of material, reducing the hadronic punch-through background to a negligible level. This region does, however, face a large combinatoric background due to the flux of beam jet related particles. There are on average 6 to 14 hits per plane in a given bunch crossing, and the drift tubes near the beam axis have an approximate 5% occupancy.

The data used in this analysis come from special runs taken at low instantaneous luminosity during the 1994-95 collider run. The integrated luminosity for these runs is $104 \pm 6 \text{ nb}^{-1}$. The trigger required the presence of an inelastic collision near the center of the detector and at least one track in the SAMUS detector with an apparent $p_T^\mu > 3 \text{ GeV}/c$ pointing back to the interaction region. Muon candidates were also required to have an associated energy deposition in the calorimeter. The hit multiplicity in each layer was also required to fall below a maximum cutoff to improve background rejection and lower the trigger rates to an acceptable level.

Muons are selected offline in the rapidity range $2.4 < |y^\mu| < 3.2$, with $p^\mu < 150 \text{ GeV}/c$ and $p_T^\mu > 2 \text{ GeV}/c$. Single interaction events are selected by requiring only one reconstructed vertex in an event, leaving an effective integrated luminosity of $\mathcal{L} = 75 \pm 7 \text{ nb}^{-1}$. Muon tracks are required to have at least 15, out of an average of 18, hits. To ensure a good momentum measurement, we require muons to traverse a magnetic field integral of at least 1.2 T·m. Muons are also required to be associated with a track-like object in the calorimeter with energy deposition consistent with that of a minimum ionizing particle. With these cuts, the combinatoric background is determined using both data and Monte Carlo (MC) to be less than 1%. The number of surviving muons in this sample is $N^\mu = 5106$.

The muon trigger and track reconstruction efficiencies are obtained using data and MC single muons, with detector simulation using GEANT [10], superimposed onto real minimum bias events. The trigger efficiencies for the hit multiplicity cut $[(31 \pm 2)\%]$ and the calorimeter confirmation $[(95 \pm 1)\%]$ are obtained from data, as are the offline cut efficiencies for energy deposition $[(94 \pm 3)\%]$ and number of hits on a track $[(96 \pm 2)\%]$. The overall detection

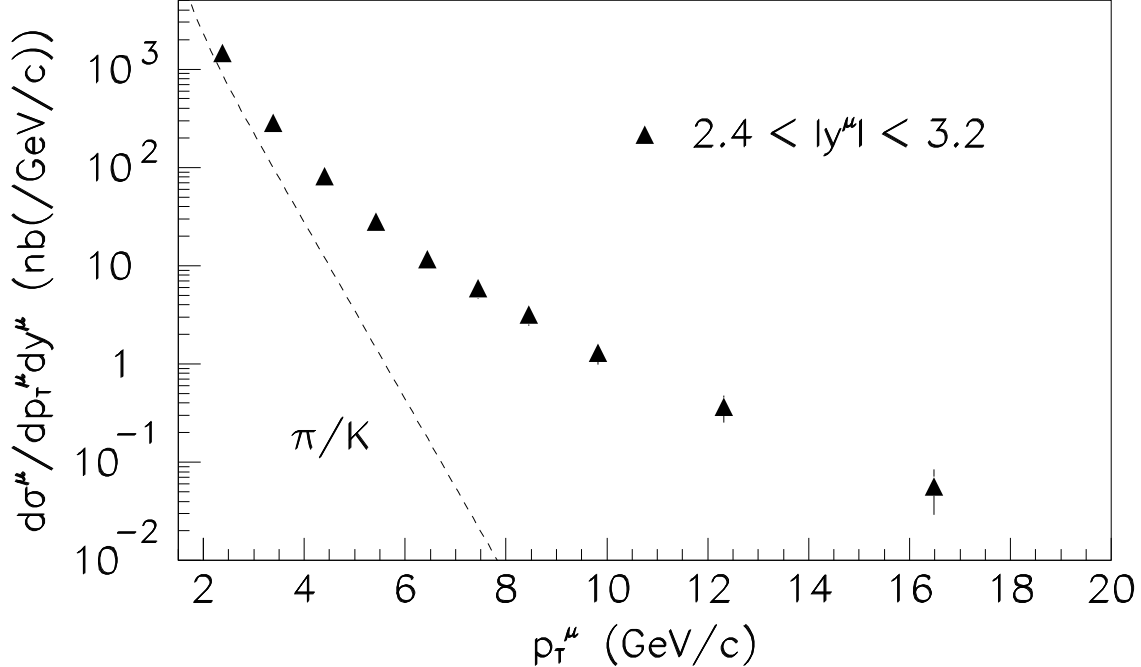


FIG. 1. The inclusive muon cross section in the forward region as a function of p_T^μ (per unit rapidity). The dashed line shows the expected contributions from π/K decays.

efficiency is 1% for $p_T^\mu = 2$ GeV/ c and reaches a plateau of 10% for $p_T^\mu > 9$ GeV/ c . The MC momentum scale and resolution are shown to be correct to within 2% by comparing the peak values and widths of the reconstructed J/ψ signal from data [9] and MC.

The muon cross section is calculated as follows:

$$\frac{d\sigma^\mu}{dp_T^\mu dy^\mu} = \frac{1}{\mathcal{L} \Delta y^\mu \Delta p_T^\mu} \frac{N^\mu f_{\text{smr}}}{\epsilon}, \quad (1)$$

where f_{smr} is a correction factor that accounts for momentum smearing, and ϵ is the detection efficiency. As there are high correlations between kinematic variables and cuts, f_{smr} and ϵ are determined by

$$\frac{N^\mu f_{\text{smr}}}{\epsilon} = \frac{1}{\epsilon_{\text{data}}} \frac{H(\text{data})H(\text{MCgen})}{H(\text{MCreco})}, \quad (2)$$

where ϵ_{data} is the combined data-based efficiency of the previously described cuts not simulated in the MC, and the H 's are matrices with elements corresponding to two-dimensional histograms in the (p_T^μ, y^μ) plane. $H(\text{data})$ is the data distribution after all offline cuts; $H(\text{MCgen})$ is the generated Monte Carlo distribution, and $H(\text{MCreco})$ is the reconstructed MC distribution with full detector simulation and the same cuts as the data. The histograms are segmented with 25 bins in p_T^μ from 0 to 25 GeV/ c , and 7 bins in rapidity from 2.0 to 3.4. The MC events are weighted in an iterative procedure to match the corrected p_T^μ and rapidity distributions of the data. This method is found to give consistent results (within 3%) regardless of the shape of the initial distribution. The resulting reconstructed MC distributions also agree quite well with those of the data for all kinematic variables of interest after the weighting procedure.

TABLE I. Forward muon cross sections (per unit rapidity).

p_T^μ (GeV/c)	$\langle p_T^\mu \rangle$ (GeV/c)	σ^μ (nb/(GeV/c))	$\sigma^\mu(\pi/K)$ (nb/(GeV/c))	f_b	σ_b^μ (nb/(GeV/c))
2 – 3	2.4	1474 ± 33 ± 265	1091 ± 383		
3 – 4	3.4	282.5 ± 7.5 ± 45	92.2 ± 33.1	0.513 ± 0.087	97.6 ± 3.8 ± 25
4 – 5	4.4	81.4 ± 3.1 ± 12	10.4 ± 3.7	0.619 ± 0.086	43.9 ± 1.9 ± 9.2
5 – 6	5.4	28.2 ± 1.5 ± 4.2	1.3 ± 0.5	0.656 ± 0.078	17.6 ± 1.0 ± 3.4
6 – 7	6.4	11.72 ± 0.80 ± 1.9	0.17 ± 0.06	0.671 ± 0.080	7.75 ± 0.54 ± 1.6
7 – 8	7.4	5.86 ± 0.53 ± 1.1	0.02 ± 0.01	0.675 ± 0.081	3.94 ± 0.36 ± 0.83
8 – 9	8.4	3.17 ± 0.34 ± 0.63		0.685 ± 0.075	2.17 ± 0.23 ± 0.50
9 – 11	9.8	1.30 ± 0.13 ± 0.29		0.697 ± 0.070	0.906 ± 0.091 ± 0.22
11 – 15	12.4	0.367 ± 0.039 ± 0.11		0.718 ± 0.067	0.264 ± 0.028 ± 0.080
15 – 20	16.7	0.057 ± 0.011 ± 0.026		0.749 ± 0.062	0.043 ± 0.008 ± 0.020

The inclusive muon cross section in the forward rapidity region (which includes both muon charges) is shown in Fig. 1 and Table I. The systematic errors in this measurement vary as a function of p_T^μ from 15 to 45%. They are dominated by uncertainties associated with the momentum smearing correction [(6–41)%], the single interaction luminosity (10%), and the trigger efficiency (8%).

The contributions to this cross section from cosmic rays, hadronic punch-through, and W/Z decay are negligible (determined using both data and MC). The pion and kaon decay contribution is obtained using ISAJET [11], which we find to be in agreement with the charged particle cross section measured in the central region [12]. The excess above the π/K contribution is attributed to b and c quark decay. The fraction of this excess due to b quark decay (f_b) can be obtained using the transverse momentum spectrum of the muons relative to that of an associated jet (p_T^{rel}), but, because of our jet reconstruction threshold of $E_T > 10$ GeV, only $(7.9 \pm 0.8)\%$ of the events in the forward region have a reconstructed associated jet. We must, therefore, rely on a NLO QCD MC to determine f_b .

In this Monte Carlo, b and c quarks are generated according to the p_T and rapidity distributions of NLO QCD calculations [4] using MRSR2 parton distribution functions [13], quark masses $m_b = 4.75$ GeV/ c^2 and $m_c = 1.6$ GeV/ c^2 , with renormalization and factorization scales $\mu = \mu_0 = \sqrt{m_q^2 + p_T^2}$. The four-momenta of the quarks are input to an ISAJET MC which simulates initial and final state radiation, as well as quark fragmentation and decay. The theoretical uncertainty is determined by varying the parameters m_b from 4.5 to 5.0 GeV/ c^2 , m_c from 1.3 to 1.9 GeV/ c^2 , and μ from $\mu_0/2$ to $2\mu_0$. The Peterson fragmentation parameters [14] ($\epsilon_b = 0.006$, $\epsilon_c = 0.06$) are also varied by 50%, as are the branching ratios within their errors [15]. This simulation predicts that 8.5% of the muons should have a reconstructed associated jet, which is consistent within errors with what is found in the data.

We check the validity of this MC by comparing its prediction for f_b to that determined from our entire 1994-95 data set. Thirty-one thousand forward muons with an associated jet are selected from low p_T single muon and muon+jet triggers. The trigger requirements keep the physics content of this sample the same as that of the cross section sample. The

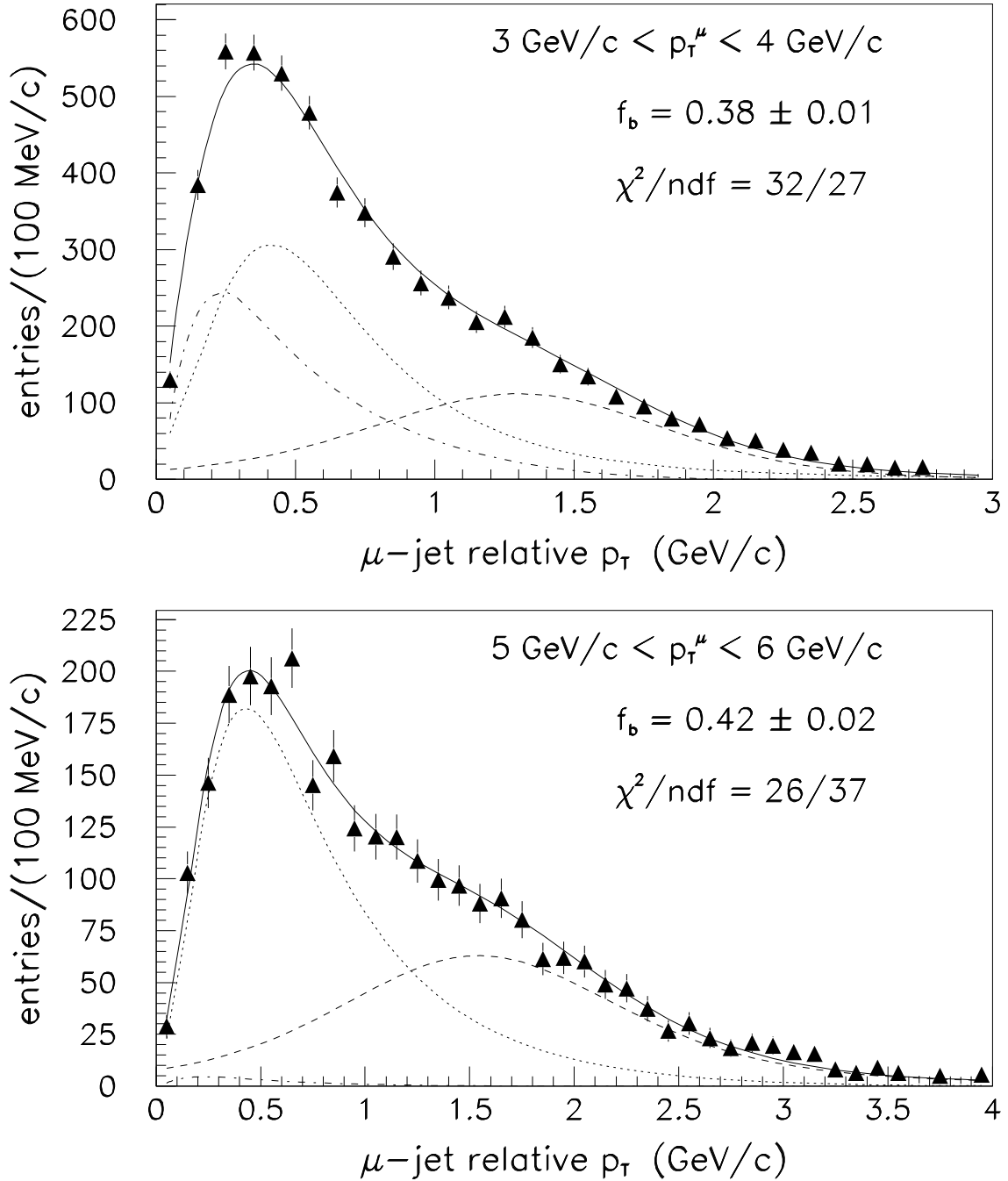


FIG. 2. Data p_T^{rel} distributions for two selected p_T^μ ranges. The solid line shows the fit to the data, with broken lines showing contributions from b quark (dashed), c quark (dotted), and π/K (dot-dashed) decay. f_b is the b quark fraction after π/K subtraction (errors are statistical only).

full sample is unsuitable for a cross section determination, however, as there is a large uncertainty in its normalization due to the various trigger thresholds and pre-scales, and luminosities that the data was taken with. The b quark fraction is determined by fitting

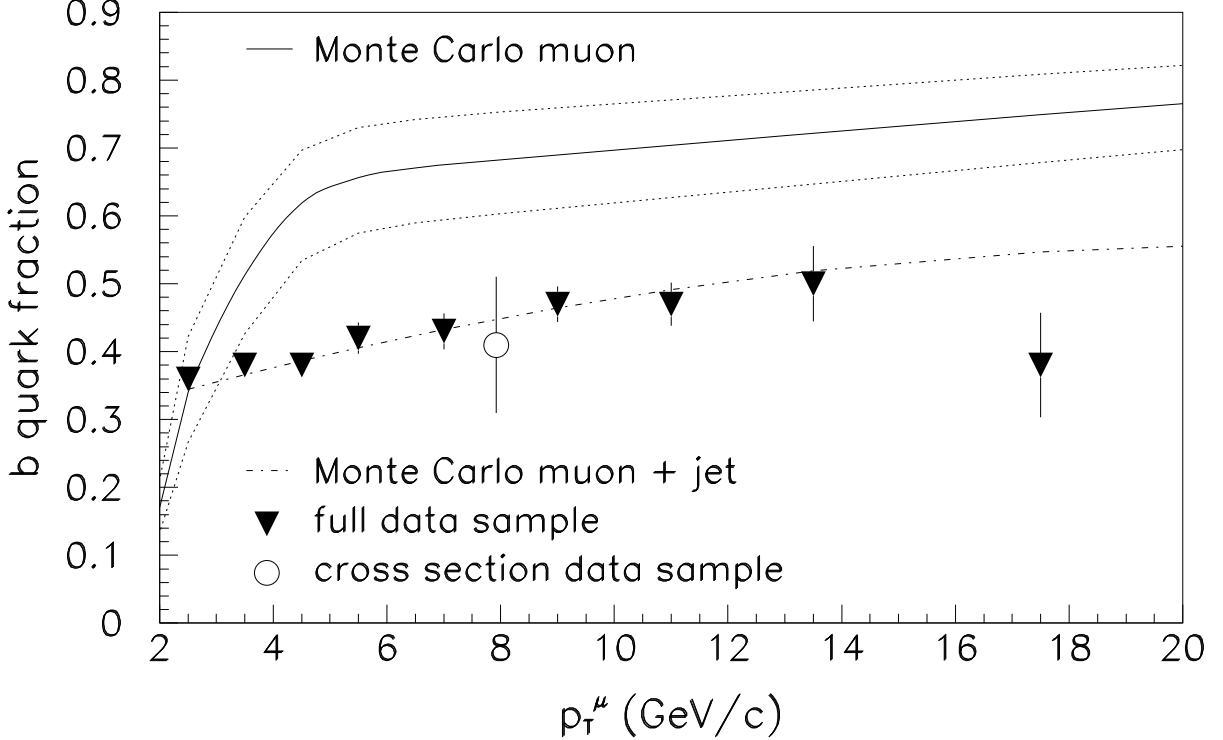


FIG. 3. f_b for muons with an associated jet as measured from data p_T^{rel} fits (triangles and circle) and as predicted by the NLO QCD MC (dot-dashed curve) The prediction of f_b for muons without the jet requirement is shown by the solid curve with uncertainties indicated by dotted curves.

the p_T^{rel} distributions (in various ranges of p_T^μ) to the expected shapes from b quark, c quark, and π/K decay (see Fig. 2) as determined from ISAJET MC. The shape for π/K decays was found to agree with the data distribution sample in the p_T^μ range 0.5–1.0 GeV/ c which is dominated by these decays. As is shown in Fig. 3, the NLO QCD Monte Carlo agrees quite well with the measured f_b obtained in the p_T^{rel} fits of both the entire data sample, and the subset of events from the cross section sample that have a jet associated with a muon. Having shown that the MC is reliable for events with muons with jets, we assume it is also reliable for inclusive muons.

Subtracting the π/K contribution from the inclusive muon cross section and multiplying the result by the QCD MC predictions for f_b gives the cross section for muons originating from b quark decay. Our measurement, which includes both muon charges, and sequential $b \rightarrow c \rightarrow \mu$ decays, is shown in Fig. 4 and Table I.

The systematic uncertainties of this measurement include those of the inclusive muon cross section, with additional uncertainties due to f_b and the π/K subtraction. The contribution to the muon cross section from π/K decay is predominantly in the low p_T^μ bins. Conservatively assuming that the data in the 2 – 3 GeV/ c bin (see Fig. 1) is entirely due to π/K decay, we determine that the ISAJET normalization is correct to within a factor of 1.35. This factor is used to determine the uncertainty in the higher p_T^μ bins.

Also shown in the figure is a cross check of our measurement. We determine the cross section using the same events, but now require the muon to be associated with a jet, and use

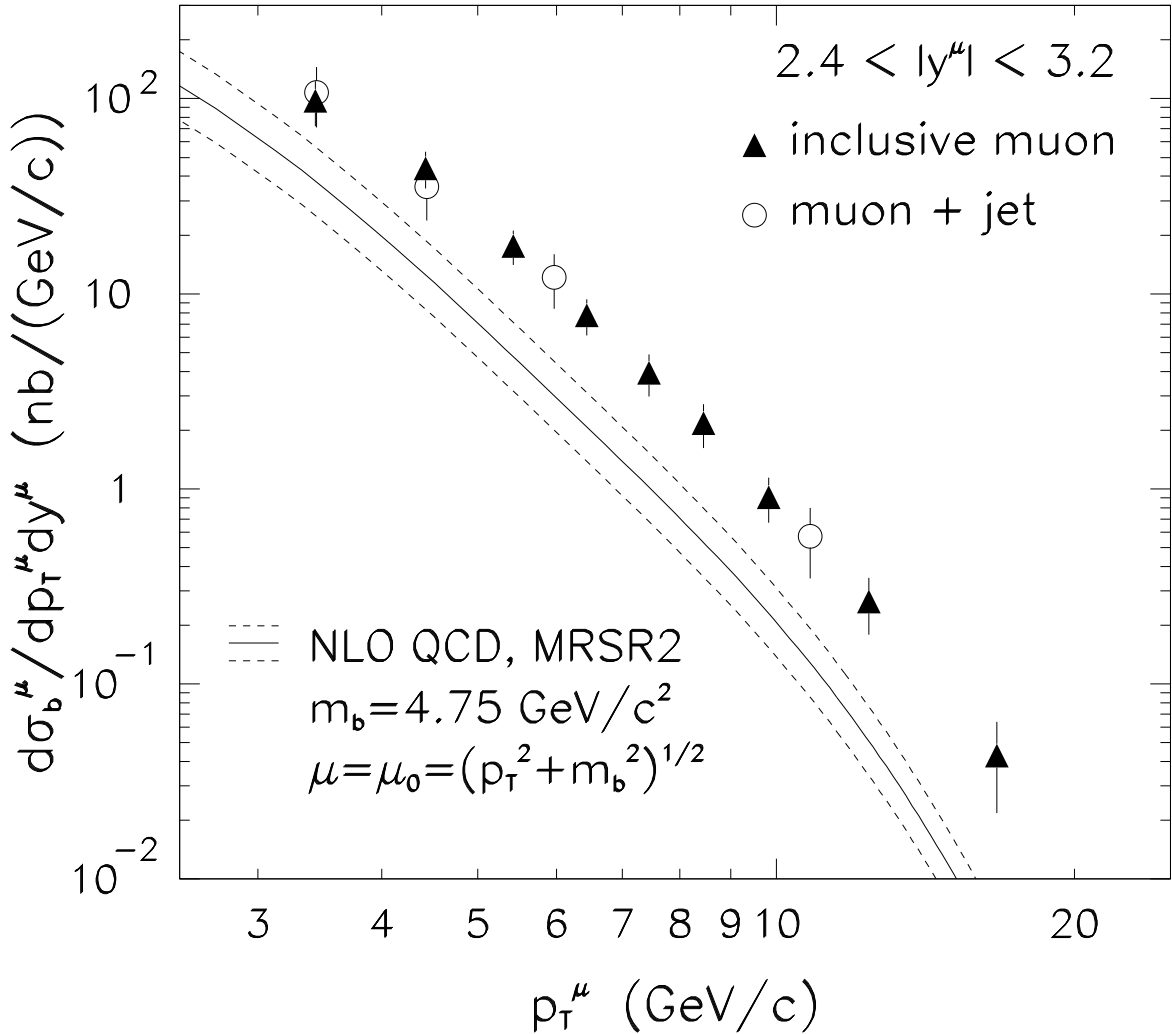


FIG. 4. The cross section for muons from b quark decay as a function of p_T^μ (per unit rapidity) as measured with the inclusive muon sample (triangles) and its sub-sample of events that have a jet associated with the muon (circles). The solid curve is the NLO QCD prediction, with the dashed curves representing the theoretical uncertainties.

the values for f_b that were determined in the p_T^{rel} fits to the entire data sample. We obtain the same cross section (within statistical errors) as we do in the inclusive muon analysis.

The NLO QCD predictions for the forward muon cross section from b quark decay are also shown in Fig. 4 as a function of p_T^μ . They match the shape of the measured cross section fairly well, but are approximately a factor of four lower than the data.

By combining the forward cross section with that of a previous $D\bar{O}$ measurement in the central rapidity range ($|y^\mu| < 0.8$) [1] we can study the rapidity dependence of b quark production. Our measurement of the cross section for muons from b quark decay as a function of rapidity ($d\sigma_b^\mu/d|y^\mu|$) is shown in Fig. 5 for both $p_T^\mu > 5 \text{ GeV}/c$ and $p_T^\mu > 8 \text{ GeV}/c$. The ratios between data and theory are shown in Table II. We find that next-to-leading order QCD calculations do not reproduce the measurements.

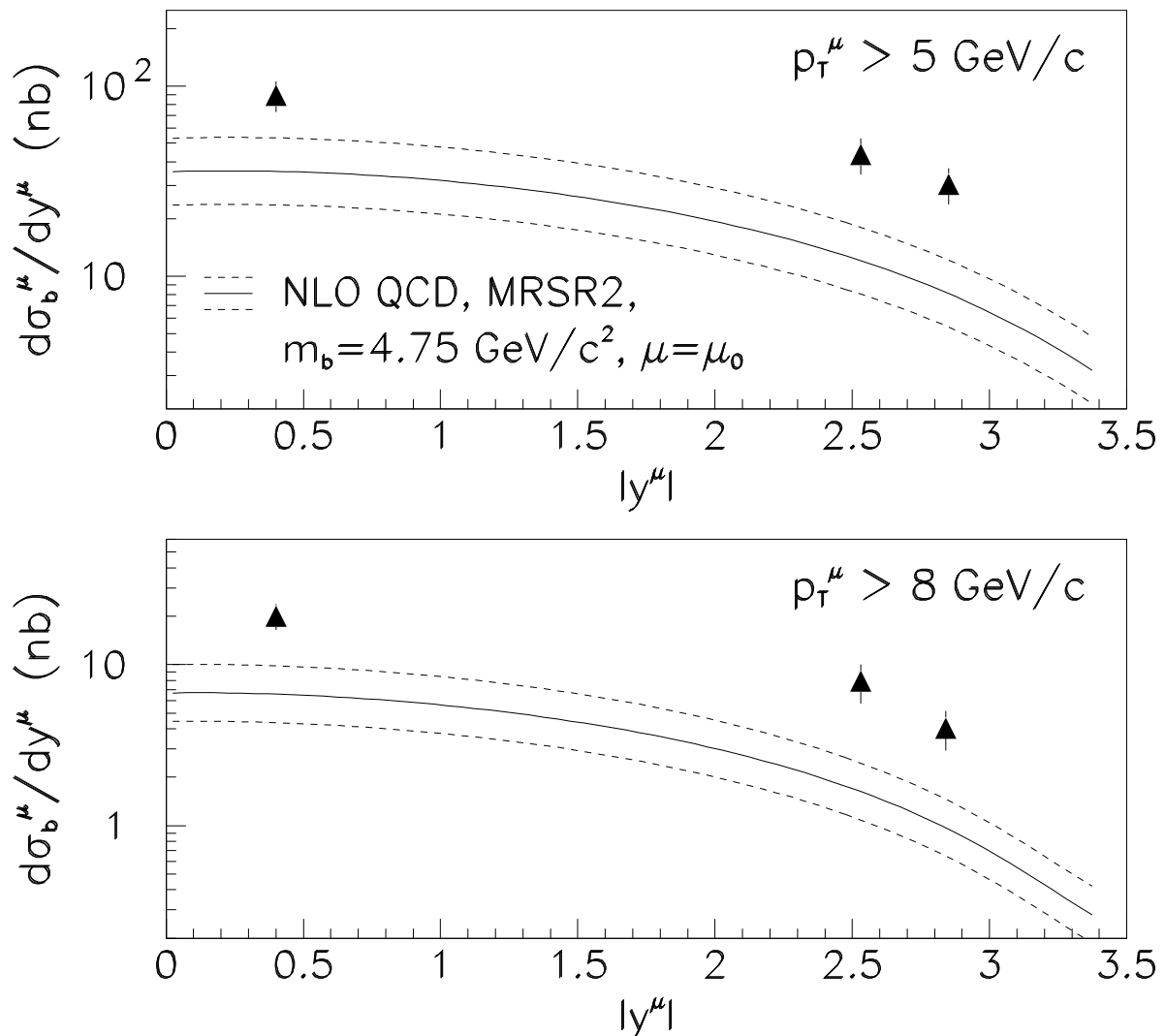


FIG. 5. The cross section of muons from b quark decay as a function of $|y^\mu|$ for $p_T^\mu > 5$ GeV/ c , and $p_T^\mu > 8$ GeV/ c . The solid curves are the NLO QCD predictions, with uncertainty bands shown by the dashed lines.

There have been some recent theoretical attempts to account for the discrepancy between data and theory. New calculations based on a variable flavor number scheme [16] predict an increase in the b quark cross section by a factor of 1.2 – 1.5 with respect to the standard calculations which use a fixed flavor number scheme. An increase in the B -meson cross section of 50% in the forward region and 30% in the central region can also be obtained by using a stiffer b quark fragmentation function than the standard Peterson form [17]. Neither of these effects, however, can bring the predicted cross sections up to the measured values.

In summary, we have measured the inclusive muon cross section, and the cross section for muons originating from b quark decay, in the forward rapidity region of $2.4 < |y^\mu| < 3.2$. We find that next-to-leading order QCD calculations underestimate b quark production by a factor of four in this region.

TABLE II. The cross section of muons from b quark decay compared to NLO QCD. Errors are statistical and systematic added in quadrature.

$p_T^\mu > 5 \text{ GeV}/c$					
rapidity	$\langle y \rangle$	measured		theory	ratio
		σ_b^μ (nb)		σ_b^μ (nb)	
0.00 – 0.80	0.40	89	± 16	36	2.5 ± 0.4
2.40 – 2.65	2.53	43.5	± 9.4	12	3.6 ± 0.8
2.65 – 3.20	2.85	30.5	± 6.6	8.4	3.6 ± 0.8

$p_T^\mu > 8 \text{ GeV}/c$					
rapidity	$\langle y \rangle$	measured		theory	ratio
		σ_b^μ (nb)		σ_b^μ (nb)	
0.00 – 0.80	0.40	20.1	± 3.7	6.6	3.0 ± 0.6
2.40 – 2.65	2.53	7.9	± 2.2	1.6	4.8 ± 1.3
2.65 – 3.20	2.84	4.1	± 1.1	0.99	4.0 ± 1.1

We thank the Fermilab and collaborating institution staffs for contributions to this work, and acknowledge support from the Department of Energy and National Science Foundation (USA), Commissariat à L’Energie Atomique (France), Ministry for Science and Technology and Ministry for Atomic Energy (Russia), CAPES and CNPq (Brazil), Departments of Atomic Energy and Science and Education (India), Colciencias (Colombia), CONACyT (Mexico), Ministry of Education and KOSEF (Korea), and CONICET and UBACyT (Argentina).

REFERENCES

- [1] S. Abachi *et al.* (DØ Collaboration), Phys. Rev. Lett. **74**, 3548 (1995).
- [2] B. Abbott *et al.* (DØ Collaboration), FERMILAB-PUB-99/144-E, to be submitted to Phys. Rev. D.
- [3] F. Abe *et al.* (CDF Collaboration), Phys. Rev. Lett. **71**, 500, 2396, 2537 (1993); Phys. Rev. Lett. **75**, 1451 (1995).
- [4] P. Nason, S. Dawson and R.K. Ellis, Nucl. Phys. **B327**, 49 (1989); M. Beenakker *et al.* Nucl. Phys. **B351**, 507 (1991); M. Mangano, P. Nason and G. Ridolfi, Nucl. Phys. **B373**, 295 (1992).
- [5] F. Abe *et al.* (CDF Collaboration), Phys. Rev. D **53**, 1051 (1996); Phys. Rev. D **55**, 2546 (1997).
- [6] F. Abe *et al.* (CDF Collaboration), FERMILAB-PUB-98/392-E, submitted to Phys. Rev. D.
- [7] S. Abachi *et al.* (DØ Collaboration), Nucl. Instrum. Methods Phys. Res., A **338**, 185 (1994).
- [8] C. Brown *et al.* (DØ Collaboration), Nucl. Instrum. Methods Phys. Res., A **279**, 331 (1989); Yu. Antipov *et al.*, Nucl. Instrum. Methods Phys. Res., A **297**, 121 (1990).
- [9] B. Abbott *et al.* (DØ Collaboration), Phys. Rev. Lett. **82**, 35 (1999).
- [10] R. Brun and F. Carminati, CERN Program Library Long Writeup W5103, 1993 (unpublished).
- [11] F. Paige and S.D. Protopopescu, BNL Report BNL-38034, 1986 (unpublished), release V7.22.
- [12] F. Abe *et al.* (CDF Collaboration), Phys. Rev. Lett. **61**, 1819 (1988).
- [13] A. Martin, R. Roberts and J.W. Stirling, Phys. Rev. D **47**, 867 (1993); **51**, 4756 (1995).
- [14] C. Peterson *et al.*, Z. Phys. C **36**, 163 (1987).
- [15] C. Caso *et al.*, Euro. Phys. J. **C3**, 1 (1998).
- [16] F. Olness, R. Scalise and Wu-Ki Tung, Phys. Rev. D **59**, 14506 (1999).
- [17] M. Mangano, CERN preprint TH-97-328, 1997 (unpublished).